Glycosylation of Erythropoietin Affects Receptor Binding Kinetics: Role of Electrostatic Interactions

Ryan J. Darling, Uma Kuchibhotla, Wolfgang Glaesner, Radmila Micanovic, Derrick R. Witcher, and John M. Beals*

BioResearch Technologies and Proteins, Lilly Research Laboratories, Eli Lilly and Co., Indianapolis, Indiana 46285

Received July 24, 2002; Revised Manuscript Received October 3, 2002

ABSTRACT: Erythropoietin (EPO) is a cytokine produced by the kidney whose function is to stimulate red blood cell production in the bone marrow. Previously, it was shown that the affinity of EPO for its receptor, EPOR, is inversely related to the sialylation of EPO carbohydrate. To better understand the properties of EPO that modulate its receptor affinity, various glycoforms were analyzed using surface plasmon resonance. The system used has been well characterized and is based on previous reports employing an EPOR-Fc chimera captured on a Protein A surface. Using three variants of EPO containing different levels of sialylation, we determined that sialic acid decreased the association rate constant (k_{on}) about 3-fold. Furthermore, glycosylated EPO had a 20-fold slower k_{on} than nonglycosylated EPO, indicating that the core carbohydrate also negatively impacted k_{on}. The effect of electrostatic forces on EPO binding was studied by measuring binding kinetics in varying NaCl concentrations. Increasing NaCl concentration resulted in a slower k_{on} while having little impact on k_{off}, suggesting that long-range electrostatic interactions are primarily important in determining the rate of association between EPO and EPOR. Furthermore, the glycosylation content (i.e., nonglycosylated vs glycosylated, sialylated vs desialylated) affected the overall sensitivities of k_{on} to [NaCl], indicating that sialic acid and the glycan itself each impact the overall effect of these electrostatic forces.

Erythropoietin (EPO)[1] is a glycoprotein hormone that stimulates erythropoiesis by binding its cognate receptor (EPOR) located primarily on erythroid progenitor cells in the bone marrow (*1*). The ultimate effect is an increase in red blood cell number. For over a decade, recombinant EPO has been used therapeutically to treat anemia secondary to renal failure, cancer chemotherapy, and HIV infection.

Native EPO contains three N-linked glycans at Asn-24, 38, and 83 and one O-linked glycan at Ser-126. This carbohydrate is important for biosynthesis and secretion (*2*), an in vivo half-life of ∼4−5 h (*3*), and physical stability (*4*, *5*). The importance of N-linked carbohydrate for in vivo bioactivity appears to be primarily due to decreasing the rate of EPO clearance. Each N-linked glycan can accommodate up to four sialic acid residues, while the O-linked glycan can contain up to two. Thus, native EPO can contain a maximum of 14 sialic acid residues. Interestingly, previous studies have demonstrated that desialylation of EPO results in an increased EPOR affinity (∼4-fold), potentially explaining why asialo-EPO has 3−4-fold greater in vitro bioactivity (*4*, *6*). In vivo, the lower affinity of heavily sialylated EPO is more than compensated for by an increased efficacy, presumably due to an extended half-life. It has generally been presumed that the increased efficacy is due solely to an increased half-life and is independent of receptor affinity. Recently, a longer-acting variant of EPO, called novel erythropoiesis stimulating protein (NESP), has been approved for therapeutic use and is distinct from EPO in that it contains two additional N-linked glycosylation sites (*7*−*10*). The higher carbohydrate and sialic acid content of NESP results in a 4.3-fold reduction in affinity for EPOR (*10*).

Despite the understanding that EPO sialylation has a negative impact on receptor binding affinity, the mechanism for this effect remains unclear. In this manuscript, we demonstrate that the reduced affinity is primarily due to a reduction in the on-rate (k_{on}), with very little change in the off-rate (k_{off}). The reduced k_{on}, the complementarily charged EPO/EPOR binding interfaces, and other studies (*11*−*18*) demonstrating that long-range electrostatic forces primarily affect k_{on} suggest that electrostatics may play a critical role in EPO/EPOR interaction. Our observation that the primary effect was on k_{on} is consistent with an electrostatic effect (*19*). This effect is referred to as electrostatic steering, as these forces can act over relatively long distances and modulate k_{on} by influencing directional diffusion.

An emerging concept about the role of electrostatics in protein association has been gained from studies involving the interaction of barnase/barstar (*11*−*14*), acetocholinesterase/fasciculin-2 (*15*), and others (*16*−*18*). The common feature is that k_{on} shows a strong dependence on ionic strength whereas k_{off} is relatively insensitive. These observations have led to the hypothesis that long-range attractive electrostatic forces, the magnitude of which are influenced by ionic strength, act to enhance k_{on}, often by several orders of magnitude. The extent of this enhancement is a function of complementarily charged binding surfaces and has facilitated the rational design of faster associating protein pairs (*11*). Because these studies involved only nonglycosylated proteins, the extent to which carbohydrate and its

* To whom correspondence should be addressed. Tel.: 317-276-1682. Fax: 317-277-8200. E-mail: BEALS_JOHN_M@lilly.com.

[1] Abbreviations: EPO, human erythropoietin; EPO-IRS, erythropoietin international reference standard; EPOR, human erythropoietin receptor; SPR, surface plasmon resonance; NGE, nonglycosylated EPO.

10.1021/bi0265022 CCC: $22.00
Published on Web 11/12/2002

associated negative charge (i.e., sialic acid) could affect electrostatic contributions is unknown. By varying NaCl concentrations to progressively shield electrostatic forces, we demonstrate that both the carbohydrate core structure and terminal sialic acid moieties negatively affect intrinsic electrostatic enhancement of k_{on}, resulting in a reduced affinity. This direct comparison of nonglycosylated EPO and glycosylated EPO (± sialic acid) provides a unique example of how both the carbohydrate core structure and sialic acid can dampen electrostatic contributions to k_{on}, while having very little effect on k_{off}. Given the importance of carbohydrate in an ever-increasing number of therapeutic proteins, these findings may aid in the rational design of improved molecular entities with significant therapeutic advantages over their natural counterparts.

EXPERIMENTAL PROCEDURES

Materials. The EPO international reference standard, referred to here as EPO-IRS, is the European Pharmacopoeia Biological Reference Preparation.

Cell Culture. 293EBNA cells were maintained in Dulbecco's modified Eagle's medium/F-12 (3:1) supplemented with 5% fetal bovine serum, 20mM HEPES, 2mM L-glutamine, 50 μg/mL Geneticin, and antibiotic−antimycotic mixture.

Construction, Expression, and Purification of EPOR-Fc. The extracellular domain of EPOR (signal sequence plus residues 1−225) and the Fc/hinge regions of human IgG1 were each amplified by PCR to generate two products with an overlapping region. The primers were designed to incorporate a Factor Xa cleavage site (IEGR) between EPOR and IgG1, but this cleavage site was not used in this study. In addition, a C5G mutation was incorporated into the Fc hinge to remove the free cysteine. Glycine was selected to replace cysteine because of its presence at the same position in IgG4 and to introduce more flexibility in the hinge. The resulting construct is referred to as EPOR-Fc.

EPOR-Fc was transiently expressed in 293EBNA cells (see *Transient Expression of EPO in 293EBNA cells* for methods), and the medium was collected. EPOR-Fc was purified by Protein A affinity chromatography using a HiTrap Protein A column (Amersham Pharmacia Biotech). EPOR-Fc was captured and washed in 20mM sodium phosphate, pH 7.0, and eluted in 0.1 M citric acid, pH 3.5. Fractions were collected at 1 min intervals, and the pH was immediately adjusted by collecting sample into tubes containing 1 M Tris−hydrochloride, pH 8. Following affinity chromatography, EPOR-Fc was further purified by size exclusion chromatography on a Superdex 200 column (Amersham Pharmacia Biotech) with phosphate buffered saline containing 0.5 M NaCl as running buffer. Fractions containing EPOR-Fc were pooled, dispensed in aliquots, and stored at −20 °C.

NGE Expression, Purification, and Refolding. NGE was expressed in bacteria, isolated from solubilized inclusion bodies, refolded, and purified by size exclusion chromatography according to previously published methods (*20*).

Transient Expression of EPO in 293EBNA Cells. Human EPO cDNA was subcloned into a cytomegalovirus expression vector and transfected into 293EBNA cells. Plasmid preparation was performed using the Maxi Plasmid Kit (Qiagen) according to the manufacturer's protocol. Cells were plated (3.0×10^6) onto 100 mm polylysine-coated plastic dishes and grown overnight to 70−80% confluency. The medium was aspirated and replaced with 10 mL of fresh medium 1−2 h before transfection. For each transfection, 73 μL FuGene (Roche Molecular Biochemicals) was added to 820 μL Opti-mem (Life Technologies, Inc.) and incubated at room temperature for 5 min. The Fugene/Opti-mem mixture was transferred to a tube containing 12 μg of plasmid and incubated at room temperature for 20 min. The resulting mixture was added dropwise to each dish of cells and incubated at 37 °C overnight. The following day, medium was aspirated, cells were rinsed twice with phosphate-buffered saline, and 10 mL of serum free medium was added. The medium was collected and replaced daily for 4−5 days. Collected media were filtered through a 0.22 μm filter, aliquoted, and frozen at −20 °C. EPO generated by this method is referred to as EPO-293.

Desialylation of EPO-IRS with Neuraminidase. Agarose beads containing immobilized Neuraminidase type VI-A (Sigma-Aldrich) were washed four times with ∼10 volumes of 0.1 M sodium acetate, pH 5.0, with centrifugation at 8000 rpm in an Eppendorf 5415C centrifuge between washes to pellet beads. Final beads were resuspended in the same buffer at 800 mU/mL. EPO-IRS was resuspended in 0.1 M sodium acetate, pH 5.0, and neuraminidase beads to give final concentration of 0.25 mg/mL EPO and 250 mU/mL neuraminidase, resulting in a 1.0 mU/μg enzyme:substrate ratio. Sample was incubated 8−10 h at 37 °C. Beads were removed by centrifugation, and the supernatant was filtered through a Millex GV 0.22 μm filter (Millipore). The sample was dialyzed against 10mM HEPES, pH 7.4, 150mM sodium chloride using a 10 000 Da molecular weight cutoff Slide-A-Lyzer (Pierce). Removal of sialic acid was confirmed by oligosaccharide profiling.

Determination of Protein Concentration. Quantitation of EPO-293 from cell media was performed by analytical reversed-phase high-performance liquid chromatography followed by peak integration and interpolation from a standard curve. Samples were injected onto a Zorbax 300SB C_8 column equilibrated to 60 °C in 10% acetonitrile/0.1% trifluoroacetic acid and eluted using a linear 10−90% acetonitrile gradient over 15 min (flow rate = 1.0 mL/min). Absorbance was monitored at 214 nm. The accuracy of this method (error <5%) was determined by spiking mock-transfected cell medium with known concentrations of EPO. Concentrations of EPO-IRS, asialo-EPO, and NGE were determined by absorbance at 280 nm using an extinction coefficient of 1.248 cm^2/mg. Concentrations of NGE−Lys and NGE−Glu were determined by absorbance at 280 nm using an extinction coefficient of 1.243 cm^2/mg.

Oligosaccharide Profiling. The extent of sialylation was determined using a modified protocol based on a previous report (*21*). The sample (∼30 μg protein) was denatured in 0.75 M Tris−hydrochloride, pH 8.1, 4 M urea, 5 mM dithiothreitol at 37 °C for 20 min at a final protein concentration of ∼0.15 mg/mL. To alkylate free thiol groups was added 5.0 μL of 0.54 M iodoacetic acid, and the mixture was incubated for 20 min at room temperature in the dark. The sample was desalted over Bio-Gel P-6 gel column (Bio-Rad Laboratories) equilibrated with 10 mM ammonium bicarbonate to give a final volume of 300 μL. To release oligosaccharides, 0.2 units of N-glycanase (Glyco, Inc.) were added, and samples were incubated 15−18 h at 37 °C. After incubation, 3 μL of 10% acetic acid was added and the sample was centrifuged for 5 min at 6000 rpm. The recovered supernatant was dried in vacuo.

Fluorescent labeling of oligosaccharides was performed using reagents in a Signal 2AB Labeling Kit (Glyco, Inc. #K-404). A 150 μL aliquot of glacial acetic acid (vial C) was added to DMSO (vial B) and mixed. A 100 μL aliquot of the resulting solution was added to the 2-aminobenzamide (vial A) and mixed. The solution in vial A was added to a reductant (vial D), mixed, and used to label oligosaccharides. After labeling, 2.0 μL of the above solution was added to each dried oligosaccharide sample, mixed thoroughly, and incubated at 65 °C for 2 h. The sample was allowed to cool to room temperature, and excess labeling reagent was removed by passage through a 0.5 mL bed of P-2 Bio-Gel (Bio-Rad Laboratories). The sample was eluted in a final volume of 250 μL water and dried in vacuo.

Oligosaccharides were resuspended in 25 μL of water and analyzed by anion exchange chromatography. A 10 μL aliquot was injected onto a DEAE-5PW column (7.5 mm × 7.5 cm, Tosohaas) equilibrated with 5% acetonitrile, pH 9.0 (buffer A), at a flow rate of 0.8 mL/min. The following gradient, with 5% acetonitrile/0.5 M ammonium acetate, pH 8.0, as buffer B, was used: isocratic elution for 10 min at 0% buffer B, followed by a linear gradient of 0−20% B over 50 min. Fluorescence was detected with excitation and emission wavelengths of 330 and 420 nm, respectively. Asialo, mono-, di-, tri-, and tetrasialylated oligosaccharides were quantitated by peak integration according to previously reported peak assignments (*21*). To confirm that nearly all associated charge of the carbohydrates was due to sialylation, 10 μL of each sample was desialylated prior to DEAE chromatography. Less than 5% of the oligosaccharides contained charge not removed by neuraminidase.

Surface Plasmon Resonance (BIAcore). Surface plasmon resonance measurements were performed on a BIAcore 2000 instrument containing a B1 sensor chip. Protein A (Calbiochem, La Jolla, CA) was immobilized onto flow cells 1 and 2 using amine-coupling chemistry. Flow cells were activated for 7 min with a 1:1 mixture of 0.1 M N-hydroxysuccinimide and 0.1 M 3-(*N*,*N*-dimethylamino)propyl-*N*-ethylcarbodiimide at a flow rate of 5 μL/min. Protein A (30 μg/mL in 10mM sodium acetate, pH 4.5) was injected over both flow cells for 15 min at 5 μL/min, which resulted in a surface density of 700−800 response units (RU). Surfaces were blocked with a 7 min injection of 1 M ethanolamine−HCl, pH 8.5. To ensure complete removal of any noncovalently bound Protein A, 15 μL of 10mM glycine, pH 1.5 was injected twice. The running buffer used for kinetic experiments contained 10mM HEPES, pH 7.4, 50−1000 mM NaCl, 0.005% P20, and 0.1 mg/mL bovine serum albumin (BSA). BSA was included to minimize nonspecific protein adsorption at dilute concentrations (*22*).

EPO/EPOR-Fc binding and BIAcore analysis have been previously described in detail (*22*). Consistent with this previous study, EPO interaction with EPOR-Fc was partially limited by mass transport. Thus, collection of kinetic binding data was performed at maximum flow rate (100 μL/min) and a low surface density to minimize mass transport effects. All experiments were performed at 25 °C. Each analysis cycle consisted of (i) capture of 140−150 RU EPOR-Fc by injection of 15−20 μL of 40 nM EPOR-Fc (108 kDa) over flow cell 2, (ii) 2 min stabilization time, (iii) 250 μL injection of EPO (concentration range of 8 nM to 0.0625 nM in 2-fold dilution increments) over flow cells 1 and 2 with flow cell 1 as the reference flow cell, (iv) 10 min dissociation (buffer flow), (v) regeneration of Protein A surface with a 30 s injection of 10mM glycine, pH1.5 at 20 μL/min, (vi) a 45 s blank injection of running buffer at 20 μL/min, and (vii) a 2 min stabilization time before start of next cycle. Signal was monitored as flow cell 2 minus flow cell 1. Samples and a buffer blank were injected in triplicate in a random order. k_{on} and k_{off} were simultaneously fit to a 1:1 binding with mass transport model (*22*) using global data analysis in BIAevaluation 3.1 software.

Table 1: Quantitation of Sialic Acid Content of EPO Isoforms[a]

EPO form	sialic acid species: asialo (%)	mono (%)	di (%)	tri (%)	tetra (%)	mol sialic acid/mol glycan[b]	mol sialic acid/mol protein[c]
EPO-IRS	0.5	3.0	15	37	44	3.2	9.6
EPO-293	20	24	23	22	11	1.8	5.4
Asialo-EPO	90	4.9	4.3	1.0	0	0.17	0.5

[a] Sialic acid content of N-linked carbohydrates was quantitated as described in Experimental Procedures. [b] Calculated as ((% mono × 1) + (% di × 2) + (% tri × 3) + (% tetra × 4))/100. [c] Calculated by multiplying mol sialic acid/mol glycan × 3 mol glycan/mol protein.

Electrostatic Contribution to k_{on}. Previous studies involving association of hirudin/thrombin (*23*), acetylcholinesterase/fasciculin (*23*), barnase/barstar (*11*, *23*, *24*), interferon α2/receptor (*18*), TEM1 β-lactamase/BLIP (*12*), and associated mutants have shown that electrostatic contributions to binding can be determined by measuring k_{on} as a function of salt concentration. A linear relationship between k_{on} and ionic strength is related to the Debye−Hückel energy of interaction according to the following equation (*23*, *24*):

$$\ln k_{on} = \ln k_{on}^{\circ} - \frac{U}{RT}\left(\frac{1}{1+\kappa a}\right)$$

where k_{on}° and k_{on} are on rates in the absence and presence of electrostatic forces, respectively, U is the electrostatic energy of interaction, R is the gas constant, T is temperature, "a" is the minimal distance of approach set to 6 Å, and κ is the Debye−Hückel screening parameter that relates to ionic strength. Accordingly, a plot of ln k_{on} versus $(1 + \kappa a)^{-1}$ yields a straight line with a slope of $-U/RT$ and the y-intercept equal to ln k_{on}°. U is interpreted as the electrostatic contribution of both proteins in the absence of salt, and k_{on}° is the predicted basal association rate when NaCl shields all electrostatic forces (extrapolation to infinite NaCl; $(1 + \kappa a)^{-1} = 0$). Thus, the magnitude of the slope is an indicator of the contribution that electrostatic forces make in determining k_{on}. This linear relationship has held for TEM1 β-lactamase/BLIP (*12*), interferon α2/receptor (*18*), hirudin/thrombin (*23*), barnase/barstar (*11*, *23*), and a heterodimer leucine zipper (*16*) at all concentrations of NaCl tested.

RESULTS

Sialic Acid Content of EPO Variants. Sialylation levels were determined for three forms of EPO: (i) an international reference standard, called EPO-IRS, (ii) asialo-EPO, obtained by treating EPO-IRS with neuraminidase, and (iii) EPO obtained from transient expression in 293EBNA cells, referred to here as EPO-293. To determine the extent of sialylation, carbohydrates were released with N-glycosidase F and labeled with the fluorescent probe 2-aminobenzamide. Using anion exchange chromatography to separate carbohydrates based on charge, the percentages of mono-, di-, tri-, and tetrasialylated N-linked carbohydrates were determined by peak integration and are listed in Table 1. The percentages

of each sialylation type were used to calculate the average number of sialic acid residues per protein molecule that were associated with N-linked carbohydrates. As shown in Table 1, EPO-IRS, EPO-293, and asialo-EPO contained 9.6, 5.4, and 0.5 sialic acid residues, respectively. These three forms, representing a range of species with differing sialic acid content, were further evaluated below.

Kinetics of EPO-IRS Binding. EPOR is a type I transmembrane receptor that binds EPO in a ternary complex composed of two identical EPOR molecules and one EPO molecule (*25*, *26*). To study EPO/EPOR interactions using surface plasmon resonance (SPR), an assay was designed based on a previously characterized system in which each subunit of the human IgG_1 Fc domain contains the extracellular domain of EPOR connected to its C-terminus (*22*, *27*). This EPOR-Fc chimera has facilitated biophysical characterization of EPO/EPOR interactions using techniques such as SPR, analytical ultracentrifugation, isothermal titration calorimetry, and circular dichroism (*22*, *27*). From these studies, it was shown that (i) EPO and EPOR-Fc associate to form a 1:1 complex, (ii) EPO binds EPOR-Fc with an overall affinity of ~3 pM, which is 330-fold tighter than the high-affinity site of EPO (site 1) for the soluble extracellular domain of EPOR (*28*), and (iii) EPOR-Fc is 750-fold more potent than the soluble extracellular domain of EPOR in neutralizing the in vitro biological activity of EPO (*27*). These observations provide strong evidence that EPO binds both receptor domains in EPOR-Fc. Furthermore, recent crystallographic (*29*) and cell-based studies (*30*, *31*) have provided convincing evidence that unbound EPOR can exist as preformed dimers on the cell surface, further supporting the use of this construct as a model to study EPO/EPOR interactions.

EPO-IRS was used to initially characterize binding of EPO to EPOR-Fc using SPR. To create an oriented surface, EPOR-Fc was captured onto a B1 chip containing immobilized Protein A. This capture step was followed by injection of EPO-IRS at 2.0, 1.0, 0.5, 0.25, 0.125, 0.0625, and 0 nM concentrations. A low maximum response for EPO binding (<35 RU), attained by capturing about 140 RU of EPOR-Fc, and a flow rate of 100 μL/min were used to minimize mass transport limitations (*22*). The buffer used was at physiological pH (7.4) and ionic strength (150 mM). Figure 1 shows an overlay of raw sensorgram data for different EPO concentrations performed in triplicate, demonstrating the reproducibility of the EPOR-Fc capture step and EPO binding.

Although using a low-capacity surface and high flow rates minimizes mass transport effects, these effects cannot be completely eliminated from the EPO/EPOR system (*22*). Therefore, data from the portion of the sensorgram representing EPO association and dissociation were analyzed and globally fit to a 1:1 mass transport limited model (*22*, *32*). This model includes a mass transport coefficient, K_t, which takes into account the transport of EPO to and from the sensor surface. Four independent experiments were performed and data were fit globally for each experiment. The results indicate that EPO-IRS binds EPOR-Fc with a fast association rate ($k_{on} = 2.1 \pm 0.26 \times 10^7$ M^{-1} s^{-1}) and a slow dissociation rate ($k_{off} = 7.8 \pm 0.95 \times 10^{-5}$ s^{-1}), resulting in an overall binding affinity of 3.7 pM at 25 °C (calculated from $K_D = k_{off}/k_{on}$). Figure 2A shows an overlay of the fitted curves and the data for repeat injections of six EPO concentrations. Residuals of the fit were distributed randomly about the *x*-axis (Figure 2B), indicating that the model fit well to the raw data.

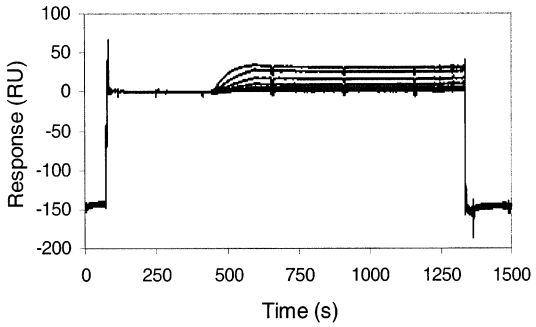

FIGURE 1: Raw sensorgram data for EPO-IRS binding to EPOR-Fc on BIAcore. Shown is an overlay of 21 sensorgrams (six concentrations of EPO-IRS and a blank, each in triplicate) with data *y*-transformed using data points prior to EPO injection. EPO concentrations used were 2.0, 1.0, 0.50, 0.25, 0.13, and 0.063 nM. The first phase of the sensorgram at 75 s is the capture of about 145 RU of EPOR-Fc onto the Protein A surface in flow cell 2. The flow is then switched to both flow cells 1 and 2, with flow cell 1 being the reference flow cell lacking EPOR-Fc. EPO-IRS injections occur from 450 to 600 s, followed by monitoring dissociation for 10 min. The final phase of the each sensorgram is a regeneration step where glycine pH 1.5 is injected to remove EPOR-Fc and EPO-IRS, leaving Protein A to be reused in subsequent cycles. Regeneration returns the RU response to baseline. The overlay of response levels for EPOR-Fc capture, EPO-IRS binding, and return to baseline indicates that the system is stable and highly reproducible.

Core Carbohydrate Structure and Sialic Acid Content of EPO Affect Binding Kinetics. As mentioned previously, it is well documented that levels of EPO sialylation are inversely related to receptor affinity (*4*, *6*, *10*). To begin characterizing the molecular basis for this observation, binding studies were performed using the various isoforms of EPO containing differing levels of sialylation (Table 1). In addition, nonglycosylated EPO (NGE) was analyzed.

The kinetic rate constants obtained for NGE, asialo-EPO, 293-EPO, and EPO-IRS are listed in Table 2. NGE had the fastest k_{on} and k_{off}; however, the major effect was on k_{on}. EPO-IRS, which is fully glycosylated and highly sialylated, had a 19-fold slower k_{on} compared to NGE. EPO-293, which contained the core carbohydrate structure with about half the sialic acid content of that on EPO-IRS, had a 6.8-fold slower k_{on}. Complete removal of sialic acid (asialo-EPO) resulted in kinetics similar to EPO-293, indicating that sialic acid levels greater than 5.4 mol sialic acid/mol protein are needed to negatively impact k_{on}. Thus, the relative ranking of association rates is NGE > asialo-EPO ≈ 293-EPO > EPO-IRS. The predominant impact on k_{on} is reflected in the overall higher affinities (K_D) of desialylated and nonglycosylated isoforms (Table 2). The higher affinity of asialo-EPO is consistent with previous reports that asialo-EPO has a greater in vitro bioactivity than highly sialylated EPO (*4*, *6*) and thus provides further evidence that EPO binding to EPOR-Fc is representative of what occurs at the cell surface. In contrast to the changes observed for various EPO sialylation variants, no difference in binding was observed when sialic acid was removed from EPOR, which contains one N-linked carbohydrate (data not shown). A lack of effect of EPOR glycosylation was expected given the distal location of the single N-linked carbohydrate with respect to the binding sites.

Role of Electrostatics in EPO/EPOR-Fc Binding. Several lines of evidence suggested that the reduced k_{on} caused by

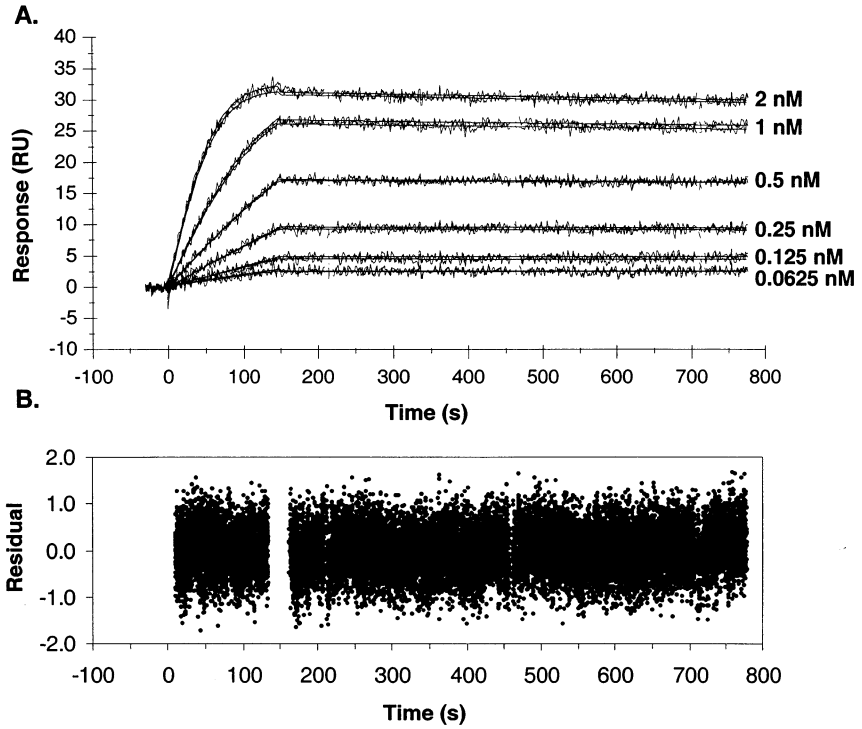

FIGURE 2: Sensorgram data and global analysis of EPO-IRS binding to EPOR-Fc. EPO-IRS (2.0, 1.0, 0.5, 0.25, 0.125, 0.0625 nM) was injected over a control surface (no EPOR-Fc), and a surface containing ~145 RU of captured EPOR-Fc and dissociation was monitored for 10 min. (A) EPO association and dissociation phases shown in duplicate for each concentration. The association and dissociation phases were globally fit to a 1:1 mass transport limited model (*22*, *27*). The fit of the data is shown as a solid line. Parameter values obtained are listed in Table 2. (B) Residuals for the global fit of EPO-IRS binding to EPOR-Fc.

Table 2: Kinetic Rate Constants for EPO Isoforms at $I = 150$ mM

EPO form	k_{on} (10^7) ($M^{-1}\,s^{-1}$)[a]	k_{on} decrease (fold)[b]	k_{off} (10^{-5}) (s^{-1})[a]	k_{off} decrease (fold)[b]	K_D (pM)[c]
NGE	40 ± 4	−	28 ± 4	−	0.7 ± 0.1
Asialo-EPO	5.9 ± 0.05	6.8 ± 0.8	14 ± 3	2.0 ± 0.4	2.4 ± 0.4
EPO-293	5.4 ± 0.4	7.4 ± 0.9	11 ± 0.7	2.5 ± 0.3	2.0 ± 0.2
EPO-IRS	2.1 ± 0.3	19 ± 3	7.8 ± 1	3.6 ± 0.5	3.7 ± 0.6

[a] Mean ± S.E.M. for 3−4 independent experiments that were each fit globally. [b] Relative to NGE. [c] Calculated from k_{off}/k_{on}.

glycosylation and, in particular, sialic acid, could be electrostatic in nature. First, the rapid on rate (10^7−10^8 M^{-1} s^{-1}) was considerably greater than the limit predicted by rotational and translational diffusion (~10^5 M^{-1} s^{-1}) (*24*), suggesting that k_{on} is enhanced by electrostatic attraction. Second, the EPOR binding surface is negatively charged, whereas EPO binding surfaces are primarily positively charged (*33*). Third, the locations of sialic acid and carbohydrates on EPO suggest that the carbohydrates project away from the binding interfaces; this distal orientation suggests that the effects caused by carbohydrate and associated sialic acid are long-range in nature. However, because little is known about the structural nature of the carbohydrate, it is possible that the carbohydrates could extend into the vicinity of receptor binding sites causing steric hindrance.

To determine the role of electrostatic interactions in the binding of the various EPO isoforms, SPR experiments were performed at increasing levels of NaCl to progressively shield long-range electrostatic forces. Thus, the sensitivity of k_{on} to increasing NaCl concentration is an indicator of the importance of electrostatics in determining k_{on}. As indicated in Experimental Procedures, the effect of electrostatics can be observed by plotting ln k_{on} versus $(1 + \kappa a)^{-1}$, where κ relates to ionic strength. According to theory (*11*, *12*), this plot should result in a straight line with a slope of $-U/RT$, which is related to the electrostatic energy of interaction (U). Thus, a greater slope indicates a greater dependence of k_{on} on electrostatic enhancement. The plots obtained by measuring binding kinetics at NaCl concentrations ranging from 50 mM to 1.0 M are shown in Figure 3. The data generated for each variant was fit by linear regression and resulted in R^2 values ranging from 0.96 to 1.0 (Table 3). This linear relationship has also been shown for TEM1 β-lactamase/

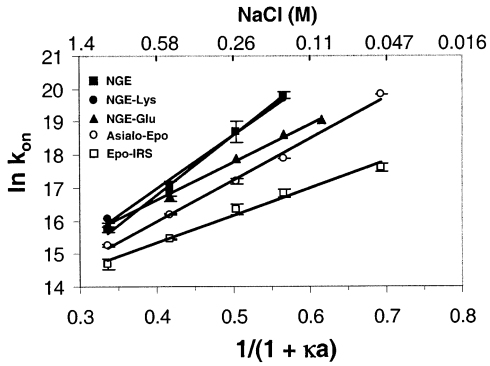

FIGURE 3: Role of electrostatic forces in EPO/EPOR-Fc interaction. The kinetics of binding to EPOR-Fc for various EPO isoforms was determined at NaCl concentrations ranging from 0.05 to 1.0 M. Data are plotted as ln k_{on} vs $(1 + \kappa a)^{-1}$, where κ relates to ionic strength (see Materials and Methods). Each data set was fit by linear regression; the slopes ($-U/RT$), which relate to the electrostatic energy of interaction, and correlation coefficients (R^2) are reported in Table 3. The values reported are the mean ± SEM for 2−4 independent experiments. The symbols are EPO-IRS (open squares), asialo-EPO (open circles), NGE (solid squares), NGE−Glu (solid triangles), and NGE−Lys (solid circles). Error bars for some points are hidden by the symbol.

Table 3: Electrostatic Contributions to k_{on}

EPO form	$-U/RT$[a]	R^2	k_{on} fold increase (1.0 → 0.15 M)[b]
NGE	18.0 ± 1	0.98[c]	58 ± 8
NGE−Lys	16.2 ± 0.9	0.98	45 ± 9
NGE−Glu	11.7 ± 0.2	1.0	15 ± 0.7
Asialo-EPO	12.6 ± 0.4	0.99	14 ± 0.3
EPO-IRS	8.3 ± 0.5	0.96	8.4 ± 2

[a] $-U/RT$ was obtained from the slopes of the lines in Figure 3. [b] Calculated from k_{on} (0.15 M NaCl)/k_{on} (1.0 M NaCl). [c] correlation coefficient from linear regression of data points in Figure 3.

BLIP (*12*), interferon α2/receptor (*18*), hirudin/thrombin (*23*), barnase/barstar (*11*, *23*), and a heterodimer leucine zipper (*16*). NGE showed the greatest electrostatic energy contribution, with $-U/RT$ equal to 18.0 ± 1.1. The presence of nonsialylated glycans (asialo-EPO) at positions 24, 38, 83, and 126 reduced $-U/RT$ to a value of 12.6. An even further decrease in $-U/RT$ was observed in the presence of sialic acid (EPO-IRS) ($-U/RT = 8.3$). The changes in values for k_{on} at 0.15 and 1 M NaCl are listed in Table 3. NGE displayed a 58-fold enhancement in k_{on} from 1 to 0.15 M NaCl, compared to an 8-fold enhancement for EPO-IRS. These results support the hypothesis that glycosylation and sialylation of EPO results in a slower k_{on} by dampening the effects of electrostatic forces.

To further investigate the electrostatic effect, NGE was produced with negative charge (NGE−Glu) or positive charge (NGE−Lys) at the four glycosylation sites. These mutants were constructed to test the effect of replacing glycans and sialic acid with surface point charges. The effects of these mutations are shown in Figure 3. The binding of NGE−Glu was significantly different than that of NGE with a reduction in $-U/RT$ from 18.0 to 11.7. This result corresponded to a ~3-fold reduction in k_{on} relative to NGE (at 150 mM NaCl), which is similar to the ~3-fold reduction in k_{on} for EPO-IRS compared to asialo-EPO. Thus, the introduction of single negative charges on the protein surface had an effect similar to that of having multiple sialic acid residues present on the termini of glycans. NGE−Lys was indistinguishable compared to NGE, indicating that the effect was specific to the negative charge in NGE−Glu.

For all variants tested, the effect of NaCl on k_{off} was minimal (Figure 4). This is consistent with data from other protein pairs suggesting that electrostatics primarily affect k_{on} because they are long-range in nature. This suggests that the rate-limiting step in dissociation of EPO/EPOR-Fc is the disruption of short-range interactions.

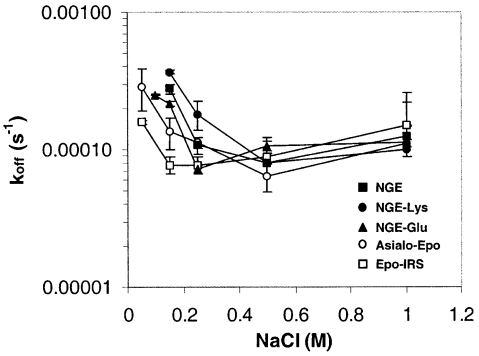

FIGURE 4: k_{off} is insensitive to shielding of electrostatic forces by NaCl. The k_{off} values, plotted as a function of NaCl concentration, were determined in the same global fittings as the values for k_{on} reported in Figure 3. The symbols are: EPO-IRS (open squares), asialo-EPO (open circles), NGE (solid squares), NGE−Glu (solid triangles), and NGE−Lys (solid circles).

DISCUSSION

Several reports have shown that long-range electrostatic interactions can dramatically enhance the rate of association between proteins, while having little or no effect on the rate of dissociation. These studies are supported by experiments that measure k_{on} as a function of increasing salt concentration, which acts to shield electrostatic forces, and mutational studies that determine the importance of charged residues in association kinetics. Both of these experimental strategies support the generalization that electrostatics primarily affect k_{on}. All of these studies, however, were performed using nonglycosylated proteins. Here, we demonstrate that electrostatic enhancement of k_{on} can be negatively influenced by both glycosylation and the negatively charged sialic acid residues associated with the glycans.

Previous studies have shown that sialylation of EPO carbohydrates results in a reduced receptor binding affinity (~3−4-fold) (*4*, *6*), but the mechanism for this effect remains uncertain. Receptor binding affinity (K_D) is a function of both k_{on} and k_{off} ($K_D = k_{off}/k_{on}$); thus, a reduced binding affinity is either due to a slower k_{on}, a faster k_{off}, or a combination thereof. In this study, kinetic binding constants were determined directly using a previously characterized surface plasmon resonance assay (*22*, *27*) that employs a soluble receptor-Fc construct. This system has the added advantage in that it is amenable to altering the solution conditions of the binding reaction; in this study, salt concentrations were varied to investigate the role of electrostatic interactions.

Our initial characterization of EPO binding to EPOR-Fc was performed using a highly sialylated form of EPO, called EPO-IRS, at physiological ionic strength (150 mM) and pH (7.4). The rate of association for EPO-IRS (2.1×10^7 M^{-1} s^{-1}) is considerably faster than most protein−protein associations, which are generally 10^5−10^6 M^{-1} s^{-1}, but significantly slower than the value of 8.1×10^7 M^{-1} s^{-1} previously reported for EPO/EPOR-Fc interaction (*22*, *27*). Knowing that processing of EPO carbohydrates can vary greatly depending on the host cell line and culture conditions, we hypothesized that the difference in k_{on} could be due to different sialylation levels. To investigate this, we analyzed asialo-EPO and EPO expressed in 293EBNA cells (EPO-293), which contained about half the number of sialic acid residues compared to EPO-IRS; both had a k_{on} that was about 3-fold faster than that of EPO-IRS and was in better agreement with the previously reported k_{on}. The similar increase in k_{on} for asialo-EPO and EPO-293 suggests that the effect of sialic acid is almost entirely due to increasing the average number of sialic acid residues from 5 to 10 and that the presence of less than five residues has no detectable effect on binding kinetics. However, because our analysis of sialic acid was global and did not measure site-specific sialylation, we cannot rule out the possible importance of the relative distribution of sialic acid residues among the carbohydrates; this possibility is currently being investigated.

Varying ionic strength conditions alters the magnitude of electrostatic forces as described by Debye−Hückel theory and can be used experimentally to determine the importance of these forces to the kinetics of a molecular interaction; the rate of a binding event for a system that is highly dependent upon electrostatic enhancement will be significantly affected by ionic strength. The effect of ionic strength can be

determined by plotting ln k_{on} versus $(1 + \kappa a)^{-1}$ to yield a linear relationship with the slope relating to the electrostatic energy of interaction (Figure 3). This linear relationship, which has been observed for several other protein systems (*11*, *12*, *16*, *18*, *23*), fits well with the EPO/EPOR-Fc data. The slope obtained for EPO-IRS was 8.3, compared to 12.6 for asialo-EPO, consistent with the effect of sialic acid being electrostatic in nature and having a negative impact on k_{on}. The difference in the magnitude of the effect on k_{on} caused by varying the NaCl concentration (EPO-IRS compared to asialo-EPO), the predominately negative binding surface of EPOR, and the slower k_{on} for EPO-IRS suggest that electrostatic repulsion between negatively charged sialic acid and EPOR is the main force that slows the rate of association. Thus, removal of sialic acid may alleviate some repulsion and allow the existing attractive forces to further enhance k_{on}.

An unanticipated result was the significantly faster k_{on} observed for nonglycosylated EPO (NGE) compared to asialo-EPO; NGE had a 6.8-fold faster k_{on} compared to asialo-EPO at $I = 150$ mM. This effect is attributed to the lack of the core carbohydrate structure on NGE. The difference in the electrostatic energies of interaction (slope of the lines in Figure 3) suggests that the effect is at least partly due to impacting electrostatics because NGE has a significantly greater slope than that of asialo-EPO. It should be noted that a nonelectrostatic effect should result in a line shifted in the vertical direction running parallel to asialo-EPO. A potential explanation for this effect is that the carbohydrate may mask or shield some of the attractive electrostatic forces present between EPO and EPOR binding surfaces and/or introduce some steric hindrance that alters association.

Interestingly, k_{on} can be slowed and the electrostatic energy of interaction reduced for NGE by introducing negative charge in the form of glutamic acid at glycosylation sites 24, 38, 83, and 126 (NGE−Glu; Figure 3). This effect was qualitatively the same as having negatively charged sialic acids on the glycan termini. In contrast, introduction of positive charge at the same sites had no observable effect. Thus, the effect of having multiple negative charges in the form of sialic acid on the glycan termini can be recapitulated by introducing negative charge at the protein surface. The fact that glycosylation sites are distal to the binding interfaces suggests that it is a global electrostatic surface potential that influences k_{on} and not solely residues directly involved in binding. This conclusion is consistent with the recent demonstration that k_{on} for TEM1 β-lactamase binding its protein inhibitor BLIP can be significantly enhanced (250-fold at $I = 22$ mM) by introducing charge mutations located outside the binding interfaces (*12*).

The linear relationship described by eq 1 allows one to estimate the basal association rate (k_{on}°) in the absence of electrostatic forces by extrapolation to infinite ionic strength (*y*-intercept), where $1/(1 + \kappa a)$ is equal to zero. In doing so, the predicted k_{on}° ranged from 1.5×10^4 M^{-1} s^{-1} for NGE to 1.6×10^5 M^{-1} s^{-1} for EPO-IRS. The reason for this difference is not apparent; however, similar results (~6-fold differences) have been obtained for other electrostatic mutations in studies involving barnase and barstar (*12*). Because of the significant extrapolation to the *y*-intercept it should be noted that small differences in the slope obtained from the region of data collection could translate into large differences at the *y*-intercept. If we assume that the variants used in this study all contain the same basal rate and constrain the *y*-intercept to a single point when fitting the data, we obtain a basal k_{on} of 7.3×10^4 M^{-1} s^{-1}, which is consistent with basal rates of other protein:protein interactions. Constraining the *y*-intercept resulted in only a slight increase in Chi^2 from 0.043 to 0.078, indicating that the constraint had only a slight impact on goodness of fit. Using 7.3×10^4 M^{-1} s^{-1} as a basal rate to calculate the electrostatic enhancement (k_{on}/k_{on}°) observed at physiological ionic strength (150 mM), k_{on} was increased 300-fold for EPO-IRS, 800-fold for asialo-EPO, and 5500-fold for NGE.

Table 4: Electrostatic Enhancement in Protein:Protein Association

protein pair	$-U/RT$[a]	ref
EPO-IRS/EPOR-Fc	8.3	−
asialo-EPO/EPOR-Fc	12.6	−
NGE/EPOR-Fc	18.0	−
TEM1/BLIP[b]	2.5−3	(*12*)
TEM1/BLIP(+6)[b,c]	11−12	(*12*)
Ifnar2/Interferon α2	4	(*18*)
barnase/barstar	7.5	(*11*, *23*)
heterodimeric leucine zipper[d]	12	(*16*)
hirudin/thrombin	13.8	(*23*, *40*)

[a] Slope of line generated from ln k_{on} vs $1/(1 + \kappa a)$ plot. [b] Value listed was estimated from data plotted in Figure 3b of ref *12*. [c] BLIP(+6) is a mutant optimized for electrostatic enhancement of k_{on}. [d] Value obtained using ionic strength and k_{on} values listed in Table 1 of ref *16* and plotted as ln k_{on} vs $1/(1 + \kappa a)$.

The role of electrostatic enhancement for EPO/EPOR compared to other well-characterized protein pairs is shown in Table 4. Comparing the slopes ($-U/RT$) obtained for the various protein pairs indicates that EPO binding to EPOR-Fc is among the highest measured to date. The glycosylated forms of EPO, having slopes of 8.3 and 12.6 for sialylated and nonsialylated forms, respectively, are considerably greater than TEM1/BLIP and IFNar2/interferon-α2 and similar to barnase/barstar, hirudin/thrombin, and a heterodimeric leucine zipper. The most rapidly binding form, NGE, with a slope of ~18, significantly exceeds all previously reported values. This result indicates that electrostatic enhancement observed for EPO binding in the absence of carbohydrate is very high compared to other proteins, and remains relatively high even in the presence of carbohydrate.

An interesting question to consider is whether the findings reported in this manuscript are unique to EPO, or are they an indication of a more common effect of glycosylation. In a previous report (*34*), Cebon et al. demonstrated that glycosylation of human granulocyte−macrophage colony stimulating factor (hGM-CSF) resulted in ~30-fold reduction in receptor affinity, which was attributed primarily to a reduction in k_{on}. Sialylation was not directly studied and the role of varying ionic strength was not possible to determine due to the cell-based assay format. Nevertheless, the primary effect of reducing k_{on} is consistent with the EPO results reported here, and suggests that a similar phenomenon may also exist for hGM-CSF binding its receptor. This notion is further supported by the fast k_{on} ($\sim 10^7$ M^{-1} s^{-1} at 4 °C) reported for nonglycosylated hGM-CSF (*34*). Glycosylation and/or sialylation have also been reported to reduce the receptor binding affinity of follicle-stimulating hormone (*35*) and luteinizing hormone (*36*); however, in contrast to EPO, hGM-CSF, and follicle-stimulating hormone, the glycans on luteinizing hormone are necessary for optimal in vitro bioactivity. To specifically determine if these effects are caused by the same mechanism as in EPO, i.e., affecting

electrostatics, biophysical studies of these systems are needed.

Clearly, EPO glycosylation and sialylation is critical to reduce the rate of in vivo clearance. The primary mechanism for this effect is mainly to prevent hepatic and renal clearance. Recent studies have provided strong evidence that ~80% of EPO's clearance is mediated by an unidentified component in the bone marrow (*37*, *38*). A likely candidate for this unidentified component is EPOR because the bone marrow is the primary site of EPOR expression and EPOR is known to internalize and degrade EPO. Thus, it is possible that receptor-mediated clearance would be reduced according to the extent of EPO sialylation. This is an intriguing prospect given the recent development of novel erythropoiesis stimulating protein (NESP), a long-acting form of EPO, which contains two additional engineered N-linked carbohydrates (up to eight additional sialic acid moieties) and a 4-fold reduction in receptor binding affinity (*7*−*10*, *39*).

The findings described here have expanded the understanding of carbohydrate effects on receptor binding kinetics for EPO and have demonstrated that both sialylation and bulk carbohydrate can negatively impact protein:protein interactions driven by electrostatic forces. This is, to our knowledge, the first report directly demonstrating that carbohydrate can have an impact on electrostatic interactions between a ligand/receptor pair. While anecdotal evidence exists suggesting that this observation may also apply to other protein pairs, more detailed biophysical studies using glycoproteins are needed.

ACKNOWLEDGMENT

The authors gratefully acknowledge Yu Tian, Joe C. Berry, Pierre-Alexandre Brault, and Rohn L. Millican for technical assistance and many useful discussions.

REFERENCES

1. Krantz, S. B. (1991) *Blood 77*, 419−34.
2. Dube, S., Fisher, J. W., and Powell, J. S. (1988) *J. Biol. Chem. 263*, 17516−21.
3. Salmonson, T., Danielson, B. G., and Wikstrom, B. (1990) *Br. J. Clin. Pharmacol. 29*, 709−13.
4. Tsuda, E., Kawanishi, G., Ueda, M., Masuda, S., and Sasaki, R. (1990) *Eur. J. Biochem. 188*, 405−11.
5. Narhi, L. O., Arakawa, T., Aoki, K. H., Elmore, R., Rohde, M. F., Boone, T., and Strickland, T. W. (1991) *J. Biol. Chem. 266*, 23022−6.
6. Takeuchi, M., Takasaki, S., Shimada, M., and Kobata, A. (1990) *J. Biol. Chem. 265*, 12127−30.
7. Smith, R. E., Jr., Jaiyesimi, I. A., Meza, L. A., Tchekmedyian, N. S., Chan, D., Griffith, H., Brosman, S., Bukowski, R., Murdoch, M., Rarick, M., Saven, A., Colowick, A. B., Fleishman, A., Gayko, U., and Glaspy, J. (2001) *Br. J. Cancer 84, Suppl. 1*, 24−30.
8. Heatherington, A. C., Schuller, J., and Mercer, A. J. (2001) *Br. J. Cancer 84, Suppl. 1*, 11−6.
9. Glaspy, J., Jadeja, J. S., Justice, G., Kessler, J., Richards, D., Schwartzberg, L., Rigas, J., Kuter, D., Harmon, D., Prow, D., Demetri, G., Gordon, D., Arseneau, J., Saven, A., Hynes, H., Boccia, R., O'Byrne, J., and Colowick, A. B. (2001) *Br. J. Cancer 84, Suppl. 1*, 17−23.
10. Egrie, J. C., and Browne, J. K. (2001) *Br. J. Cancer 84 Suppl 1*, 3−10.
11. Schreiber, G., and Fersht, A. R. (1996) *Nat. Struct. Biol. 3*, 427−31.
12. Selzer, T., Albeck, S., and Schreiber, G. (2000) *Nat. Struct. Biol. 7*, 537−41.
13. Frisch, C., Fersht, A. R., and Schreiber, G. (2001) *J. Mol. Biol. 308*, 69−77.
14. Lee, L. P., and Tidor, B. (2001) *Protein Sci. 10*, 362−77.
15. Radic, Z., Kirchhoff, P. D., Quinn, D. M., McCammon, J. A., and Taylor, P. (1997) *J. Biol. Chem. 272*, 23265−77.
16. Wendt, H., Leder, L., Harma, H., Jelesarov, I., Baici, A., and Bosshard, H. R. (1997) *Biochemistry 36*, 204−13.
17. Shen, B. J., Hage, T., and Sebald, W. (1996) *Eur. J. Biochem. 240*, 252−61.
18. Piehler, J., and Schreiber, G. (1999) *J. Mol. Biol. 289*, 57−67.
19. Zhou, H. X. (2001) *Biopolymers 59*, 427−33.
20. Beals, J. M., Glaesner, W., Micanovic, R., Millican, R. L., and Witcher, D. R. (2000) Patent WO0032772A2.
21. Kanazawa, K., Ashida, K., Itoh, M., Nagai, H., Sasaki, H., and Fukuda, M. (1999) *Biol. Pharm. Bull. 22*, 339−46.
22. Morton, T. A., and Myszka, D. G. (1998) *Methods Enzymol. 295*, 268−94.
23. Selzer, T., and Schreiber, G. (1999) *J. Mol. Biol. 287*, 409−19.
24. Vijayakumar, M., Wong, K. Y., Schreiber, G., Fersht, A. R., Szabo, A., and Zhou, H. X. (1998) *J. Mol. Biol. 278*, 1015−24.
25. Lodish, H. F., Hilton, D. J., Klingmuller, U., Watowich, S. S., and Wu, H. (1995) *Cold Spring Harbor Symp. Quant. Biol. 60*, 93−104.
26. Youssoufian, H., Longmore, G., Neumann, D., Yoshimura, A., and Lodish, H. F. (1993) *Blood 81*, 2223−36.
27. Hensley, P., Doyle, M. L., Myszka, D. G., Woody, R. W., Brigham-Burke, M. R., Erickson-Miller, C. L., Griffin, C. A., Jones, C. S., McNulty, D. E., O'Brien, S. P., Amegadzie, B. Y., MacKenzie, L., Ryan, M. D., and Young, P. R. (2000) *Methods Enzymol. 323*, 177−207.
28. Philo, J. S., Aoki, K. H., Arakawa, T., Narhi, L. O., and Wen, J. (1996) *Biochemistry 35*, 1681−91.
29. Livnah, O., Stura, E. A., Middleton, S. A., Johnson, D. L., Jolliffe, L. K., and Wilson, I. A. (1999) *Science 283*, 987−90.
30. Remy, I., Wilson, I. A., and Michnick, S. W. (1999) *Science 283*, 990−3.
31. Constantinescu, S. N., Keren, T., Socolovsky, M., Nam, H., Henis, Y. I., and Lodish, H. F. (2001) *Proc. Natl. Acad. Sci. U.S.A. 98*, 4379−84.
32. Myszka, D. G., He, X., Dembo, M., Morton, T. A., and Goldstein, B. (1998) *Biophys. J. 75*, 583−94.
33. Syed, R. S., Reid, S. W., Li, C., Cheetham, J. C., Aoki, K. H., Liu, B., Zhan, H., Osslund, T. D., Chirino, A. J., Zhang, J., Finer-Moore, J., Elliott, S., Sitney, K., Katz, B. A., Matthews, D. J., Wendoloski, J. J., Egrie, J., and Stroud, R. M. (1998) *Nature 395*, 511−6.
34. Cebon, J., Nicola, N., Ward, M., Gardner, I., Dempsey, P., Layton, J., Duhrsen, U., Burgess, A. W., Nice, E., and Morstyn, G. (1990) *J. Biol. Chem. 265*, 4483−91.
35. Zambrano, E., Zarinan, T., Olivares, A., Barrios-de-Tomasi, J., and Ulloa-Aguirre, A. (1999) *Endocrine 10*, 113-21.
36. Liu, W. K., Young, J. D., and Ward, D. N. (1984) *Mol. Cell Endocrinol. 37*, 29−39.
37. Chapel, S., Veng-Pedersen, P., Hohl, R. J., Schmidt, R. L., McGuire, E. M., and Widness, J. A. (2001) *J. Pharmacol. Exp. Ther. 298*, 820−4.
38. Chapel, S. H., Veng-Pedersen, P., Schmidt, R. L., and Widness, J. A. (2001) *Exp. Hematol. 29*, 425−31.
39. Nissenson, A. R. (2001) *Am. J. Kidney Dis. 38*, 1390−7.
40. Stone, S. R., Dennis, S., and Hofsteenge, J. (1989) *Biochemistry 28*, 6857−63.

BI0265022